Cell Reports
Physical Science

CellPress
OPEN ACCESS

Article

Energy harvesting based on compressive stress-induced ferroelectric/ferroelastic switching in polycrystalline ferroelectric materials

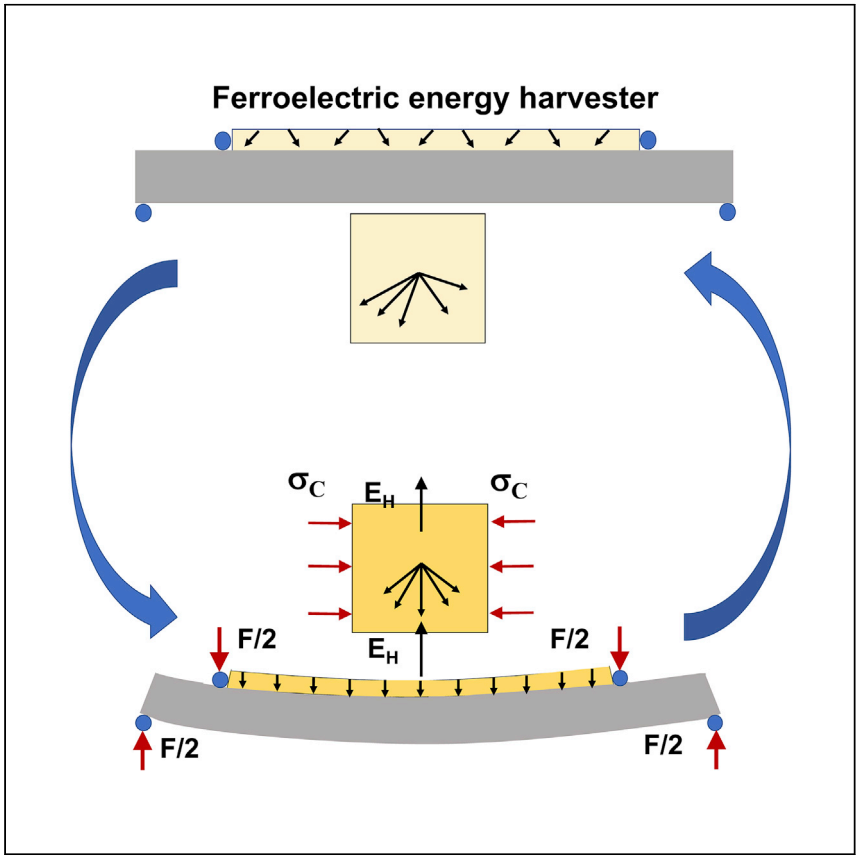

Ferroelectric/ferroelastic switching can be used for energy harvesting due to the greater energy density and charge flows than piezoelectrics. By controlling the state of polarization and residual stress, Kang and Huber report an energy harvesting method with a simple configuration that can generate a power density of 2 mW cm^{-3} at low frequency, making it a competitive substitute for piezoelectrics and triboelectrics. The device is driven by compressive loading only, avoiding fracture and fatigue degradation.

Wenbin Kang, John E. Huber

wenbin.kang@eng.ox.ac.uk (W.K.)
john.huber@eng.ox.ac.uk (J.E.H.)

Highlights

An energy harvesting cycle based on ferroelectric switching is established

A partially polarized electroceramic is developed to generate residual fields

Compressive stress only is used to drive the cycles maintaining stability

The cycle energy density reaches 2 mJ cm^{-3}, greater than piezoelectric transducers

Kang & Huber, Cell Reports Physical Science 3, 100707
January 19, 2022
https://doi.org/10.1016/j.xcrp.2021.100707

Cell Reports
Physical Science

CellPress
OPEN ACCESS

Article

Energy harvesting based on compressive stress-induced ferroelectric/ferroelastic switching in polycrystalline ferroelectric materials

Wenbin Kang[1,*] and John E. Huber[1,2,*]

SUMMARY

Although piezoelectric energy harvesting is well established, ferroelectric/ferroelastic switching has not been widely used for energy harvesting. The main disadvantage of piezoelectric energy harvesters is their limited power density. In this respect, ferroelectric/ferroelastic switching is attractive because of the greater energies and charge flows involved. However, the associated nonlinearities and the difficulty of establishing a stable working cycle have prevented significant progress. In this work, a robust ferroelectric energy harvester based on partial ferroelectric switching is explored. The device is of simple construction and achieves a per-cycle energy density of about 1 mJ cm^{-3}, orders of magnitude greater than that of typical piezoelectrics. It is shown that only periodic compressive stress is needed to induce the energy harvesting cycles, yielding promising mechanical attributes that limit fatigue or fracture during cyclic loading. The results show this prototype device operating stably over 0.5×10^6 cycles at 20-Hz frequency, demonstrating promise for practical applications.

INTRODUCTION

The last two decades have witnessed the rapid development of miniaturized portable electronics, including sensors, actuators, and the internet of things, now widely found in daily life and industry.[1–3] However, the resulting power demands are challenging for battery technologies and form a critical part of the compromise between lifetime, stability, capacity, and the practical requirements of limited size for power sources.[1–10] Therefore, energy harvesting transducers have become attractive as an alternative or supplement to batteries in portable, remote, and implantable devices. A range of energy harvesting technologies have been developed, generating electrical energy from ambient sources such as solar,[11,12] thermal,[13,14] and mechanical/kinetic energy.[15–18] These devices can save the costs and time associated with periodic recharging or replacement of batteries and can also improve sustainability.[7,10,19] Given the ubiquitous presence in nature and artificial structures of mechanical vibrations, electromechanical energy harvesters using mechanical or kinetic energy created by vehicles, human motion, ocean waves, wind, and fluids,[20–23] are widely investigated.

There are various transduction mechanisms for converting mechanical/kinetic energy to electrical energy, including piezoelectric,[24,25] electromagnetic,[26] and electrostatic.[27,28] Among these methods, piezoelectric energy harvesting has become widespread, and several researchers have attempted to optimize performance by employing materials with high piezoelectric coefficients[29] or devising advantageous

[1]Department of Engineering Science, University of Oxford, Oxford OX1 3PJ, UK

[2]Lead contact

*Correspondence:
wenbin.kang@eng.ox.ac.uk (W.K.),
john.huber@eng.ox.ac.uk (J.E.H.)

https://doi.org/10.1016/j.xcrp.2021.100707

working modes.[30,31] For example, a nickel-niobium-lead zirconate titanate (PNN-PZT) ceramic with a high piezoelectric coefficient of 1753 pC N^{-1} was proposed by Gao et al.,[32] with energy output greater than traditional PZT materials. Similarly, improved efficiency was achieved using single crystal lead magnesium niobate-lead titanate (PMN-PT) by Shahab et al.[33] and Yang and Zu[34] Using aligned PZT nanowires[35] enabled increased power density, while employing a lead titanate material enabled energy harvesting with elevated environment temperature.[36] Polymeric piezoelectrics have also been employed, particularly polyvinylidene fluoride (PVDF).[37] Datta et al.[38] reported self-poled Nylon-11 with high piezoelectricity for energy harvesting, with a wide range of temperature and excellent fatigue performance.

An alternative transduction mechanism for scavenging mechanical energy, triboelectric energy harvesting,[39,40] has becomes a hot topic since the first triboelectric nanogenerator was proposed by Fan et al.[41] in 2012; this used Kapton and polyester as triboelectric layers, in vertical contact-separation mode. Further working modes were subsequently investigated.[42,43] Hinchet et al.[44] developed an implantable device using capacitive triboelectric technology, converting the vibrational energy induced by ultrasonic sound into electrical energy, which is comparable with implantable piezoelectric transducers. In some designs, a ferroelectric ceramic layer was introduced to increase surface charge density and to induce charge flow across the device,[45] and ferroelectric polymer-based triboelectric devices are also adopted to stabilize and improve energy harvesting performance.[46,47] Additionally, Kim et al.[48] fabricated a $CaCu_3Ti_4O_{12}$ (CCTO) particle-based composite as the triboelectric dielectric material, whose high permittivity significantly increases the charge density and thereby improves the working performance.

While several of the energy harvesters described earlier make use of ferroelectric materials, none make direct use of ferroelectric or ferroelastic switching as a transduction mechanism. Ferroelectrics exhibit nonlinear hysteresis relating electric field, stress, strain, and electric displacement.[49–51] The nonlinearity is intrinsically related to ferroelectric/ferroelastic switching, and the hysteresis arises due to switching of domains, a process that can cause much greater charge flows than those found in piezoelectric transduction. Despite the potential of ferroelectrics for mechanical energy harvesting with high energy density, the challenges of nonlinearity, fatigue degradation, and the difficulty of driving an electrical cycle by stress have limited their use in energy harvesting applications. Bakshi et al.[52] and Chauhan et al.[53] proposed an energy harvesting method at the material level based on a modified Olsen cycle by ferroelectric switching induced by mechanical stress, showing prospective of energy conversion and storage. A few theoretical designs of ferroelectric energy harvester devices have been proposed,[54–60] but successful implementation has not yet been reported.

In this work, a practical ferroelectric energy harvester for low-frequency applications is established by exploiting partial ferroelectric/ferroelastic switching. Although the present work does not adopt new materials and structures, the main novelty is to engineer the material state of electroceramics in such a way as to make a stable ferroelectric/ferroelastic energy harvesting cycle possible using cyclic compression alone. Specifically, a partially poled electroceramic layer and stiff substrate are bonded together. The poling process is then completed, resulting in a state of residual stress in the electroceramic. A residual stress state is then induced using bending loads to manipulate the electroceramic into a partially depolarized state in which the polarization is easily modified by stress. Subsequently, bending loads are used to induce cyclic compressive stress driven by the substrate's curvature. This results in

a stable cycle of polarization changes driven by mechanical load, used to form an energy harvesting cycle. Both open-circuit and resistive load tests are explored, showing output energy density much greater than that of traditional piezoelectric energy harvesters. Fatigue tests demonstrate that the system is stable and robust.

RESULTS AND DISCUSSION

Working concept and design

As the use of ferroelectric or ferroelastic switching for energy harvesting is relatively novel, it is instructive to set out the reasons for this approach and the challenges to be overcome. Typical piezoelectrics operate in a linear regime with electric fields up to about 10^5 V m^{-1} and electric displacement changes of order 10^{-3} to 10^{-2} C m^{-2}. Hence, the electrical energy harvested per cycle is much less than 1 mJ cm^{-3}; values of 10^{-2} to 10^{-1} mJ cm^{-3} are common in high-performance piezoelectric devices. By contrast, the full cycle of ferroelectric hysteresis commonly involves field amplitudes of order 10^6 V m^{-1} and electric displacement amplitude of 0.1 to 0.6 C m^{-2}; thus, the electrical energy density is orders of magnitude greater than that of a piezoelectric cycle. If even a fraction of this energy could be extracted for useful electrical work, then a significant improvement in energy density could be achieved relative to piezoelectrics. The opportunity is clear, but the obstacles are significant: applying mechanical loading to a poled ferroelectric can depolarize it but will not normally repolarize it. Existing designs of ferroelectric transducers are single-shot devices designed to deliver a substantial pulse of electrical energy, but with no way of delivering continuous power. Thus, the main difficulty of energy harvesting using ferroelectric/ferroelastic switching is to establish a closed and robust working cycle by using stress only without external assistance. Meanwhile, the ferroelectric hysteresis entails switching of domains, a lossy process that can lead to rapid material degradation if operated cyclically.

The problem of producing a stable cycle in which polarization changes are driven by mechanical stresses is fundamental: as a second-order tensor, an applied stress does not define a vector direction and so cannot produce polarization change unless there is some vector-type state variable to define a direction. For example, an unpoled electroceramic cannot be poled by uniform stress alone. The idea of using a small value of applied electric field to bias the polarization in a preferred direction has been discussed in previous work.[59] However, this concept still leaves considerable challenges, caused by inaccuracies in the prediction of working cycles and the high tensile stresses required for switching. It is also challenging because of the requirements of a synchronized external bias electric field, which would complicate device design. Another possibility is to use a stress gradient or strain gradient to define a preferred direction, especially in thin-film devices. This relates to the flexoelectric effect, wherein the mechanical gradient field could influence the spontaneous polarization in a way analogous to electric field in ferroelectrics.[61,62] Alternatively, residual electric fields could provide the necessary "memory" of a preferred direction. This last approach is taken here. Thus, an objective of the present work is to identify a material state for a ferroelectric ceramic such that cyclic loading with stress produces a cyclic change in polarization. There are two methods demonstrating the potential mechanisms that can be used for energy harvesting based on this concept shown in Figure 1. In the concept shown in Figure 1A, a ceramic is first poled, then partially depolarized using stress; finally, the stress is cycled to effect a cycle of electric displacement. A disadvantage of this cycle is that tensile loading is required; in preliminary experiments, this was found to promote cracking of the ceramic, transverse to the tensile axis. An alternative using an elastic substrate

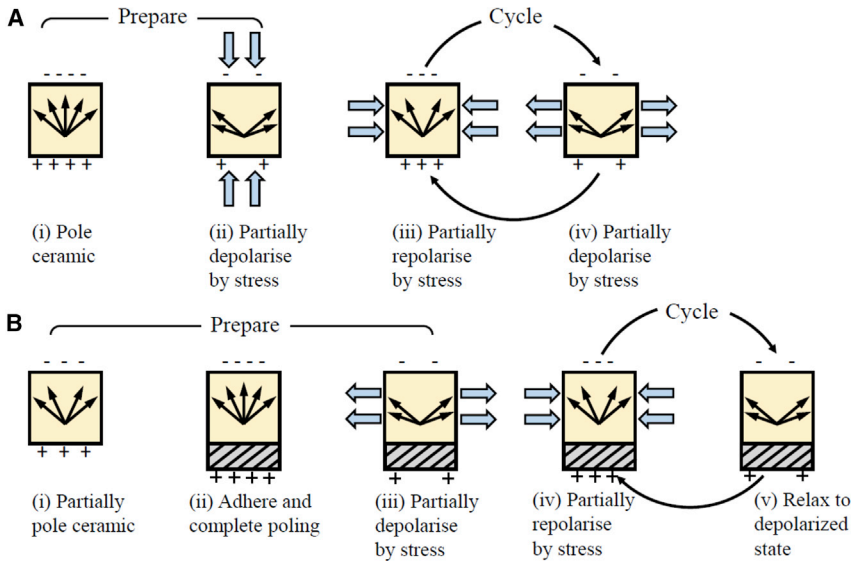

Figure 1. Preparation and working cycles for ferroelectric energy harvesting at the material level
(A) Preparation and working cycles using cyclic compressive and tensile loading.
(B) Preparation and working cycles using a substrate and cyclic compressive loading.
Black arrows indicate the polarization distribution. Hollow blue arrows indicate mechanical loading.

(shown in Figure 1B) uses only compressive loads during cycling. A residual state of tension is expected to develop in the ceramic during the cycle, but the substrate limits cracking by controlling displacement and strain in the ceramic layer. Figure 1 describes the cycle for an element of ceramic material consisting of many domains but subjected to a uniform state of loading. This demonstrates the working principle from a material perspective. Details of specimen fabrication and electrical wire connection can be found in the experimental procedures and Figure S1. Electrical energy is obtained by the movement of charges to and from the surface of the ceramic, against a voltage. The working concept of the energy harvester can be described as ferroelectric/ferroelastic switching because the polarization changes are driven by a combination of electric field and stress.

Detailed discussion of the device preparation and working cycles can be found in Note S1, wherein Figure S2 shows the device preparation and operation with a four-point bending arrangement that generates uniform stress along the device.

Results of quasi-static and vibrational tests

The proposed device arrangement could be made using a variety of existing compositions of ferroelectric. Here, 8/65/35 lanthanum doped lead zirconate titanate (PLZT) was chosen as the ferroelectric material for its low coercive field, high polarization, and fine grain size. A tool-steel substrate was used. Quasi-static tests were set up on a Deben microtester using a four-point bending fixture. For dynamic testing, a hydraulic test machine with displacement feedback by a linear variable differential transformer (LVDT) was used. The detailed specimen fabrication and test arrangements can be found in the experimental procedures.

A range of experimental conditions were considered in the tests. For example, 30%–100% prepoled specimens were prepared for energy harvesting investigation. The influences of varying mechanical load, electrical load, and frequency on energy

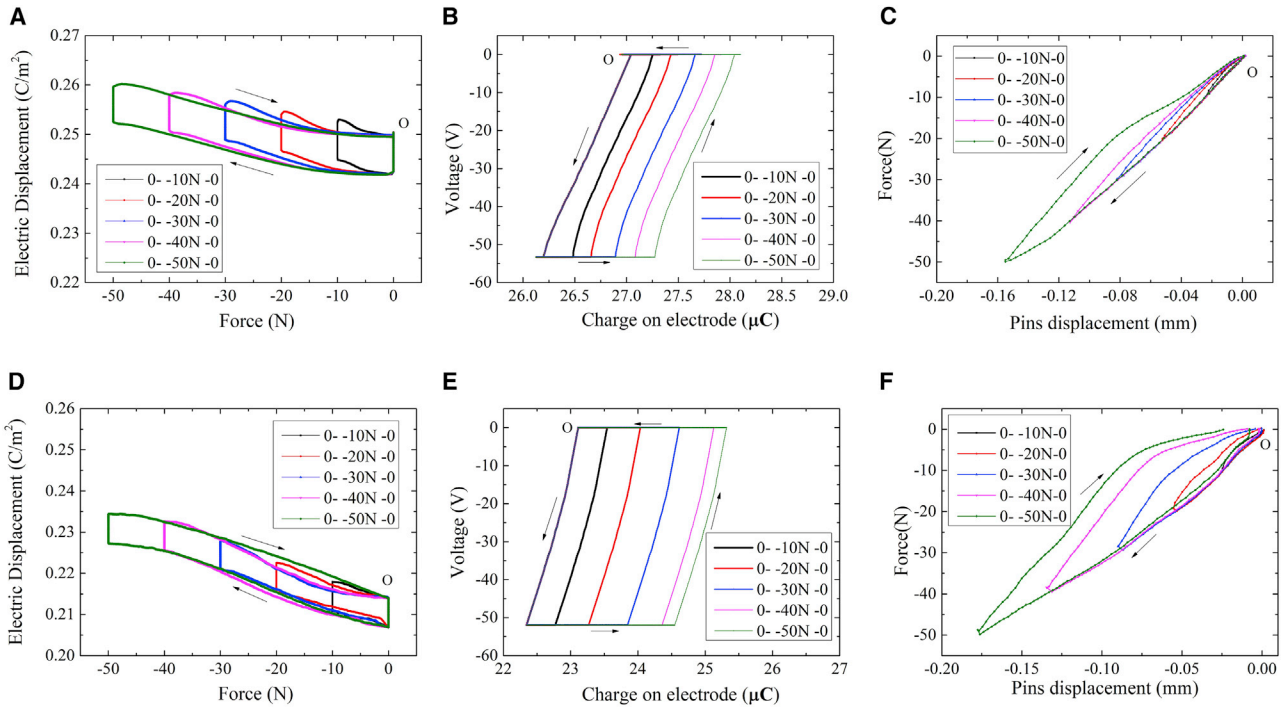

Figure 2. Comparison of the 100% prepoled and 30% prepoled energy harvesting cycles

(A–C) Energy harvesting cycles for the 100% prepoled specimen.

(D–F) Energy harvesting cycles for the 30% prepoled specimen.

(A and D) Electric displacement versus applied bending force with electric field of 0.4 E_0 applied during the energy harvesting cycle.

(B and E) Corresponding voltage versus charge cycle.

(C and F) Corresponding force versus loading pin displacement.

harvesting were also studied. Here, a limited set of results is reported in order to convey the main findings.

Quasi-static tests

Quasi-static loading tests were carried out by taking the energy harvester through the following cycle. A voltage V_{app} was first applied to the device to produce an electric field αE_0, where $E_0 = 0.36\text{MV m}^{-1}$ is the coercive field and α is a factor that could be varied to represent different electrical loads. With this electric field held constant, mechanical loading force $F/2$ was applied at each pin; total force magnitude F could also be varied to modify the cycle. The force was applied in such a way as to cause in-plane compression in the active layer, and thus drive an increase in net polarization, against the applied electric field. Next, with the loading pins held fixed, the applied voltage was reduced to zero. Finally, the mechanical load was reduced to zero. The quasi-static cycle was traversed at a frequency of 10^{-2} Hz.

For brevity, only the results for $\alpha = -0.4$ ($V_{app} = -50$ V) with the 100% prepoled and 30% prepoled samples are included here (Figure 2). The start of the cycle is marked "O" in Figures 2A–2F. The peak force value F was varied in the range from -10 to -50 N. In Figure 2A, vertical straight segments in each cycle correspond to the changes in electric displacement at constant force, due to switching the electric field "on" or "off"; curved segments correspond to the application or removal of mechanical loading. The cycle is traversed in a clockwise direction. Conversely, in Figure 2B, horizontal straight segments are seen, due to the application or removal of

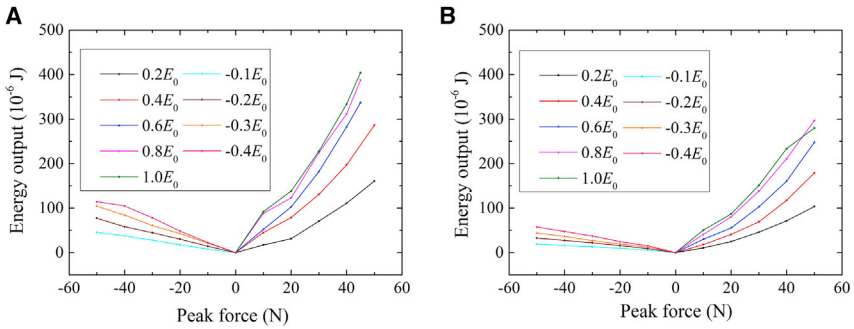

Figure 3. Energy output per cycle in quasi-static tests with tensile and compressive loading

(A) Energy output per cycle for the 30% prepoled samples.

(B) Energy output per cycle for the 100% prepoled samples.

mechanical load at constant voltage; curved segments show the variation of surface charge as the electric field is switched. Here the cycle is traversed in an anticlockwise direction. In the 100% prepoled sample, very little ferroelastic switching is expected when the mechanical load is applied because the starting state is close to a saturated, fully polarized state. The magnitude of the electric displacement changes during mechanical loading is less than 10^{-2} C m^{-2}, comparable with what is typically achieved in piezoelectric energy harvesting. By comparison, the cycles shown in Figures 2D–2F for the 30% prepoled sample are similar in character, but with much greater changes in electric displacement when mechanical loading is applied. This is consistent with ferroelastic switching caused by the mechanical loading; the cycle starts with a polarization of about 0.21 C m^{-2}, so there is freedom for the polarization to increase under mechanical loading. The enclosed area in the voltage-charge loops indicates the electrical energy output per cycle of loading. This is more than twice as great in the 30% prepoled case than in the 100% prepoled case, indicating the importance of the partial poling process. The input mechanical energy can be ascertained from the enclosed area in the force-displacement curves in Figures 2C and 2F; this grows with applied load amplitude and is much greater in the 30% prepoled case.

Figure 2 clearly demonstrates a working cycle for the ferroelectric/ferroelastic energy harvester, but it leaves open the question of how to optimize performance. There are several compromises to consider: increasing the electric field by controlling α enhances the energy output per cycle; but if the field strength becomes too high, it may cause ferroelectric switching and destroy the engineered state of the energy harvester. For this reason, experimentation was constrained to $\alpha > -0.4$. Similarly, increasing the total applied force F increases the energy per cycle, but again high values may disturb the material state by permanent ferroelastic switching, or may promote fatigue. Figure 3 summarizes results for the energy output per cycle from a set of tests in which α and F were varied in both the 100% and 30% prepoled samples.

The tests with $F > 0$ indicate cases where the sample was inverted in the loading fixture in order to produce in-plane tensile stresses in the active layer. It is found that the 30% prepoled sample consistently produces greater energy output than that with 100% prepoling. The 30% prepoled sample generated about 120 μJ per cycle with $F = -50$ N and $\alpha = -0.4$, which is much greater than that of typical piezoelectric energy harvesters. Even greater energy yields were achieved in tests

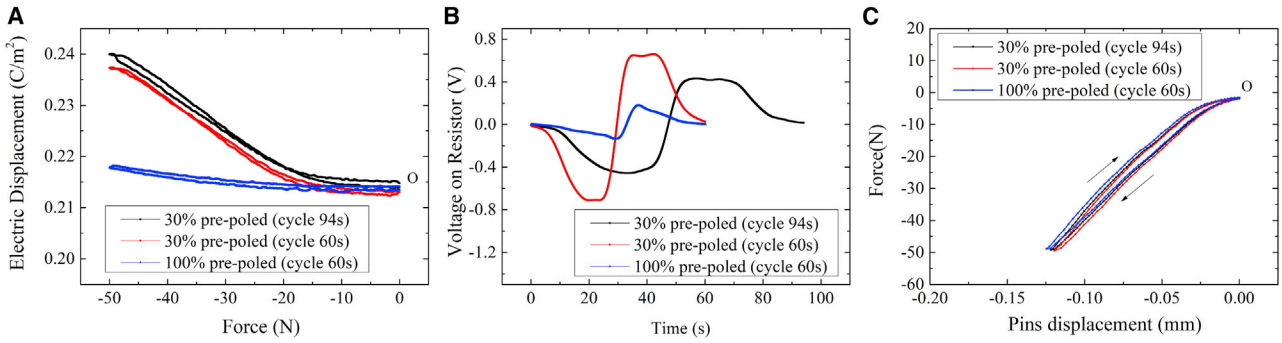

Figure 4. Quasi-static cycles with 4.620-MΩ resistive load

(A) Electric displacement versus force.

(B) Voltage versus time.

(C) Force versus displacement of loading pins.

with in-plane tension, but this mode of operation was observed to cause cracking in some cases, specifically, for $\alpha > 0.8$ and $F = 50$ N. Because the PLZT layer was translucent, the formation of cracks could be observed as lines of dark contrast when the sample was backlit.

In practical applications, it is typically the case that the voltages on an energy harvester are not controlled directly, but rather they arise due to the impedance of an external circuit. To simulate this working condition, quasi-static tests were carried out for the case $F = -50$ N with a 4.62-MΩ external load resistor (Figure 4). Once again, the 100% and 30% prepoled cases are compared. The 30% prepoled sample was also tested using two different cycle times (94 s and 60 s). The force-electric displacement cycles in Figure 4A show that the 30% prepoled sample produces much greater, nonlinear changes in electric displacement compared to the 100% prepoled case. This further confirms that ferroelectric/ferroelastic switching is occurring in the device.

The cycle period has limited effect on the electric displacement changes but does affect the voltage across the device and hence the current flow (Figure 4B). This could result in complex interactions between the device and the external circuit if the electric field in the device approaches the coercive field. Hence, control of the external electrical load and both the cyclic frequency and amplitude of mechanical loading are critical for establishing a stable energy harvesting cycle. Even in Figure 4, where the mechanical loading waveform is triangular and the voltages remain well below coercive levels, it is evident that the waveform of the generated voltage is not triangular and is dependent on frequency.

Energy harvesting performance at low frequencies

Generally, human motion can generate vibrations in a frequency range of 0.5–15 Hz, while 15- to 50-Hz vibrations are common in vehicles.[63] To test the response of the energy harvester at these frequencies, an in-house hydraulic test rig was used, and variation of prepoling states, load resistor, and frequency was explored. The mechanical displacement waveform was sinusoidal in these tests. The results presented here are a small selection intended to convey the main findings.

Figure 5 presents the effect of frequency on the 30% prepoled energy harvester, driven with 50-N force amplitude in compression, and working against a 4.67-MΩ

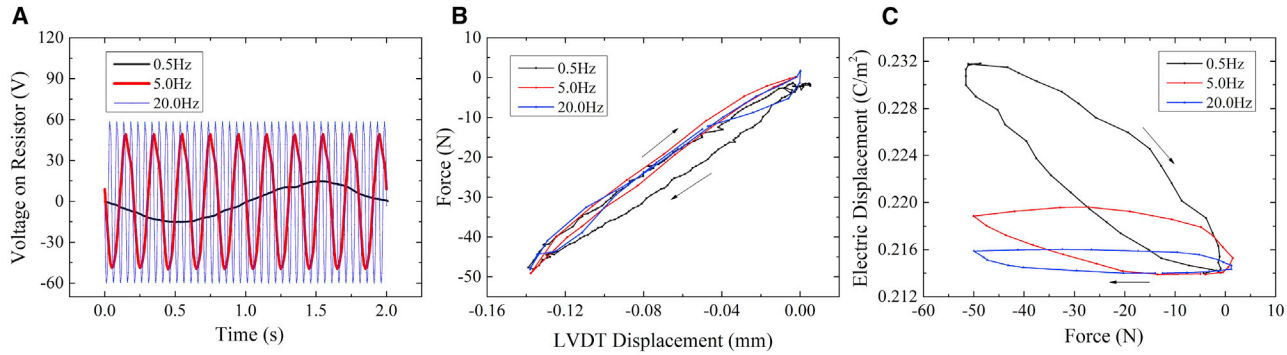

Figure 5. The 30% prepoled energy harvester tested at various frequencies

(A) Voltage across the energy harvester versus time.

(B) Force versus linear variable differential transformer (LVDT) displacement.

(C) Electric displacement versus force.

electrical load. Figure 5A shows that the generated voltage amplitude increases with frequency, although the increase from 5 to 20 Hz is only a few percent and further tests indicate that the generated voltage amplitude stabilizes as frequency increases. The generated voltage waveform is not sinusoidal, indicating nonlinearity. The electric displacement changes during each cycle at 0.5 Hz are slightly less in magnitude than the corresponding values in the quasi-static tests; the electric displacement amplitude reduces with increasing frequency. This is expected because high rates of electric displacement require high currents and hence high voltages, which in turn resist ferroelectric/ferroelastic switching. Thus, the electrical load tends to stabilize the voltage amplitude and limit switching at higher frequencies.

Figure S3 provides a performance comparison between the 30% prepoled and 100% prepoled energy harvesters operating at 20 Hz. As with the quasi-static tests, the 30% prepoled specimen demonstrates greater voltage and electric displacement amplitude—hence, greater power output. As discussed earlier, some operating conditions caused the formation of cracks in the active layer, running perpendicular to the x-axis direction. However, these cracks did not greatly affect energy harvesting performance, as seen in Figure S3, where results for both an uncracked and a cracked sample are shown. Tests were also carried out to establish whether the performance was sensitive to the sample preparation process. It was found that the results were repeatable across different samples, to within a few percent. Note that the force measurements in Figure S3B show a lack of smoothness; this appears to be an artifact of the load cell accuracy when operating at 20-Hz frequency, which was approximately ± 3 N.

It is of interest to optimize the electrical load for maximum power output. Figure 6 shows the peak voltage, electric displacement change, peak power output, and average power output of energy harvesters using 1.1-, 1.6-, and 4.67-MΩ load resistors at a range of frequencies. The peak voltages increase monotonically with frequency, whereas the electric displacement amplitude decreases monotonically. Variation of the load resistor changes the *RC* time constant and hence affects power matching. This is seen in Figure 6B where the 4.67-MΩ resistor achieves greatest power for frequencies less than 3 Hz, the 1.6-MΩ resistor achieves greatest power from 3 to 10 Hz, and then the 1.1-MΩ resistor becomes preferable for frequencies greater than 10 Hz. Because the voltage waveform varies, the average power is not directly

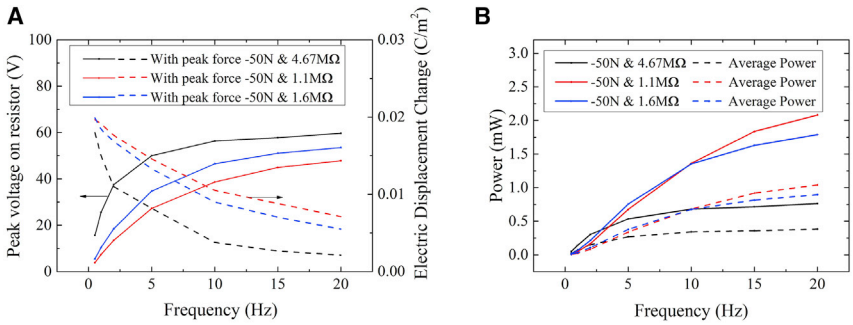

Figure 6. The effect of frequency on peak voltage, electric displacement change, and power output

(A) The effect of frequency on peak voltage and electric displacement change of the 30% prepoled specimen with 1.1, 1.6, and 4.67 MΩ.

(B) The effect of frequency on power output and average power output of the 30% prepoled specimen with 1.1, 1.6, and 4.67 MΩ.

given, as for piezoelectric harvesters, by $V^2/2R$.[64] Instead, the average power values in Figure 6B were computed by integration of the instantaneous power over the cycle. The average power shows a similar trend to the peak power data.

For practical applications, the energy harvester should be able to operate cyclically without degradation. Fatigue tests were run in various operating conditions, up to 0.5×10^6 cycles; results for a 30% prepoled sample loaded to 50 N at 20 Hz are shown in Figure S4. Following a bedding-in period, the output voltage and force-displacement cycle remained reasonably stable over the course of these tests, as seen in Figures S4A and S4B. The output voltage amplitude was found to drop by approximately 10% in the first 10^5 cycles, with a corresponding 20% drop in peak power (Figure S4C). Beyond 2×10^5 cycles, the power output appears stable. No cracks were observed in the active layer, demonstrating the stability and robustness of this ferroelectric energy harvester. The fatigue test indicates that the mechanical loads do not induce material degradation. Another important factor is the stability of the partially poled state. It is well known that the poled state of electroceramic may decay over long time periods (e.g., 10–15 years). But there is currently little evidence to show the stability of polarization in partially poled electroceramics. This may affect the energy output of the energy harvester over time and is a subject of future investigation. Additionally, the quality of bond between the substrate and active material, which induces the residual stress in the poling process, should be considered. The stressed state may relax over time or after a larger number of loading cycles. In the present work, we have observed only a small change in performance with cycling, but further work is needed to confirm the stability of the substrate-ferroelectric bond.

The frequency-power performances of various high-power vibration energy harvesters are shown in Figure 7. The ultimate objective of the present work is to improve upon the energy and power density of existing piezoelectric energy harvesting technologies. Figure 7 indicates that the ferroelectric/ferroelastic energy harvester in the present work compares favorably with a range of piezoelectric devices,[65–72] offering greater cycle energy density and greater power. The device remains effective at low frequencies, typical of structural and mechanical vibrations as well as human motion. The device has comparable cycle energy density to triboelectric energy harvesters.[73–76] Here it should be noted that some triboelectric

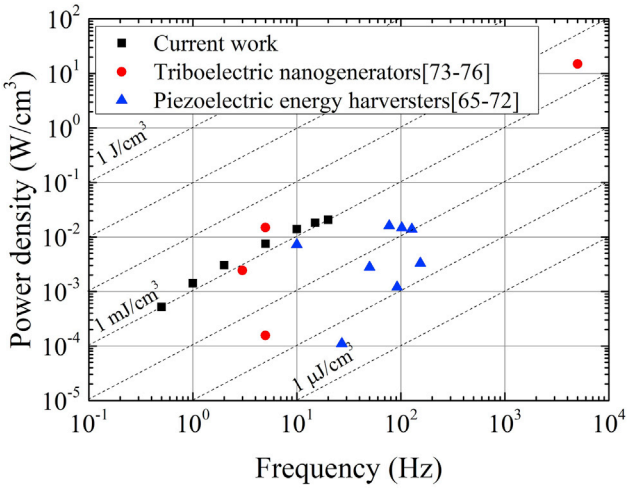

Figure 7. Frequency-power characteristics

Frequency-power characteristic for various energy harvesters.[65–76] Lines of constant cycle work density are shown. Numbers in brackets refer to references.

devices are characterized by sliding velocity rather than operating frequency and the comparison with oscillating devices has been made by assuming an amplitude and calculating the frequency that provides the required peak velocity at that amplitude. The amplitude used for comparison purposes was the amplitude of displacement applied to the loading pins in our experiment. Although the force/pressure is also of great importance for energy harvesting, the differences of loading and operation systems of all types of energy harvesters inhibit a comparison of energy output per unit force. By contrast, the peak loads used in the present work are constant. As for triboelectric energy harvesters, the cycle energy densities vary widely and can exceed that offered by the ferroelectric energy harvester in its current implementation. Specifically, the ferroelectric energy harvester presented here achieved a maximum cycle energy density in the region of 2 mJ cm^{-3}. Power output varies with frequency and was about 20 mW cm^{-3} at 20 Hz, the maximum frequency tested here.

In the present work, the ferroelectric energy harvester has not been optimized for a particular application so that the strategy can be universally applied to a range of energy harvesting applications, such as wireless sensors, medical devices, and mobile electronics through specific designs. Energy output could potentially be enhanced by tailoring such designs to the requirements of the application. For future studies, there are various options for improving performance, including choice of material and geometry for the active element and substrate, control of the prepoling procedure that initializes the energy harvester, and choice of external mechanical or electrical loads. In practical vibrational applications, the selection of a suitable inertial mass and limitation of the duty cycle to prevent overload will be critical. The nature of the energy harvesting cycle is also such that a stable amplitude of mechanical loading is advantageous, which may be a limiting factor in applications with variable or unpredictable vibrations. The focus of the present work is instead to demonstrate a working ferroelectric energy harvesting cycle with high energy density and robustness against cyclic fatigue.

A novel energy harvesting method using ferroelectric/ferroelastic switching has been proposed and tested. The method works by partially depolarizing a poled

ferroelectric using a single application of tensile stress, and then using cycles of compression to vary the polarization state. A crucial feature is the control of residual stress by poling the active material in stages, first in a mechanically unconstrained state, then adhering it to a substrate before completing the poling process. The resulting energy harvesting cycles were shown to achieve much greater energy density than typical piezoelectric devices and had comparable performance with some triboelectric generators. Even greater energy density was achieved by using tensile stress states: although this mode of loading compromised robustness, it may still be useful for applications with low cycle numbers. In compression, the cycles were shown to be reasonably stable and the device remained robust up to 0.5×10^6 cycles. Further robustness verification should be tested with greater cycle numbers in the future. Given the simplicity and ease of construction of the proposed device, it is likely to be suitable for a range of applications. It is likely that significant further improvements could be made through a more extensive design study. The investigations in this study provide a preliminary demonstration of the working principle for an energy harvester using ferroelectric/ferroelastic switching and show that the concept is promising for high-power and high-energy-density vibrational energy harvesting at low frequencies.

EXPERIMENTAL PROCEDURES

Resource availability

Lead contact

Further information and requests for resources should be directed to and will be fulfilled by the lead contact, John Huber (john.huber@eng.ox.ac.uk).

Materials availability

This study did not generate new unique reagents. The materials are from a commercial company.

Data and code availability

All data associated with the study are available from the lead contact upon reasonable request.

Specimen fabrication

A ferroelectric energy harvester was implemented using 8/65/35 PLZT as the working material. The design is generic and any ferroelectric material that also exhibits ferroelastic switching could be used. By contrast, the design of the ferroelectric energy harvester, including the choice of active material, substrate, residual fields, and mechanical load amplitude should be adjusted accordingly depending on the coercive field of the active material, and thereby the energy output will be enhanced through the optimization. This design exploration has been planned for future work. In this work, the selected PLZT material, with 8% lanthanum substitution into a 65% lead zirconate and 35% lead titanate solid solution, has the advantages of low coercive field (0.36 MV m^{-1}) and a soft composition allowing ferroelastic switching at stresses of a few megapascals.[77,78] The material has a rhombohedral-tetragonal morphotropic structure and a fine grain size (~1 μm), which is advantageous in enhancing fracture toughness. The Curie temperature is 110°C[77,78] and the maximum polarization at room temperature is 0.25 C m^{-2}. The PLZT wafers used in the experiments were all taken from the same bulk sample of commercial 8/65/35 PLZT material. The sample response varied systematically and repeatably as the design parameters were varied, giving confidence that the observed performance is not due to material variability. The energy harvester was built on a tool-steel substrate of 1-mm thickness onto which a PLZT wafer of 0.33-mm thickness

was adhered with conductive adhesive (Figure S1A). A top electrode was formed using a thin coating of conductive paint. Connections were made to the substrate and top electrode using conductive epoxy. The substrate dimensions were 68 × 4 × 1 mm with the active layer covering a central portion of 38-mm length. It also shows an edge view identifying the steel substrate, adhesive, and PLZT layers. The conductive paint layer is flexible and much thinner than the PLZT and cannot be seen in this view; it is expected to have a negligible effect on the mechanical loading.

A key feature of the device design is the poling process. The ceramic layer was partially poled, by controlling electric displacement, before being adhered to the substrate. The purpose of this partial poling process in a mechanically unconstrained state was to limit the development of in-plane tensile stresses that were shown in preliminary tests to promote degradation by cracking. The degree of partial prepoling, from 0% up to 100% (relative to the full polarization of 0.25 C m^{-2}) was varied to find optimum operating conditions. Initial tests were carried out with 100%, 75%, 50%, and 30% prepoled samples. Once adhered to the steel substrate, the poling process was then completed such that the ceramic layer was fully poled to near 0.25 C m^{-2}. The results of initial tests show that an increase of prepoling level can result in a decrease of energy output per cycle, and a 30% prepoled sample can achieve a good balance between energy output and material degradation in the further poling process. Specimens fabricated with less than 30% prepoling commonly cracked during subsequent on-substrate poling. The residual stress occurring in the poling process can be estimated based on the degree of the partially prepoled state, but it has not been measured in the present work. Based on the estimation, an increase of prepoling level can reduce the residual stress in the specimens. The measurement problem is challenging due to the varying material state and domain structure. Ferroelectric switching and residual strain can be identified using X-ray diffraction,[79,80] which is planned for future work.

Quasi-static and dynamic test arrangements

The test arrangements are shown in Figures S1B–S1E. For quasi-static testing of the energy harvesting cycle, an open-circuit arrangement was used and mechanical loading was carried out using a Deben microtest system (Figures S1B and S1D). The steel substrate was connected to ground through a capacitive electrometer. At the top electrode, voltage was controlled using LabView software and a high voltage amplifier (Trek, model 20/20C). A steady voltage opposing the charge flow during the energy harvesting cycle was used to simulate electrical load. This voltage was removed during the mechanical unloading part of the cycle. In Figure S1D, the signs of force and electric field are both negative, where the electric field direction is upward and $F < 0$ indicates the cases to produce in-plane compressive stresses in the active layer. Mechanical loading was applied by four-point bending using four alumina pins in two pairs. Each pair of pins was spaced 5-mm apart with a central span of 38.5 mm experiencing uniform bending moment. Note that the pin loads were applied directly to the substrate, in end sections beyond the region where the active material was adhered. The pin positions were monitored continually using digital image correlation.

Once a quasi-static working cycle was established, the effect of loading at a range of frequencies and with a range of passive resistive loads was studied. Cyclic mechanical loading was applied using an in-house hydraulic test machine with a four-point bend loading fixture, as shown in Figure S1C. Displacement control was achieved via feedback from a LVDT. The four-point bend fixture was made from tool steel, with alumina pins, spaced as in the quasi-static experiments. The electrical circuit

included a load resistor (labeled Resistor 2 in Figure S1E), a potential divider (Resistor 1) used to infer voltage at the electrode, and a capacitive electrometer to measure charge flow. Voltages at the electrometer were kept at the millivolt level to avoid offsetting of the sample electrode voltage, which was typically 1–50 V. Resistor 2 was varied in the range of 3–15 MΩ, and the operating frequency varied from 0.5 to 20 Hz. Runs of 0.5×10^6 cycles were used to test for stability and fatigue with all data logged using LabView software.

SUPPLEMENTAL INFORMATION

Supplemental information can be found online at https://doi.org/10.1016/j.xcrp.2021.100707.

ACKNOWLEDGMENTS

The authors thank Dr. Robert Paynter and Lulu Chang for help in the experimental setup and operations. W.K. gratefully acknowledges support from the Jardine Foundation.

AUTHOR CONTRIBUTIONS

W.K. conducted the experiments and wrote the draft, and J.E.H. took part in the design work of experiments and edited the manuscript.

DECLARATION OF INTERESTS

The authors declare no competing interests.

Received: May 11, 2021
Revised: November 19, 2021
Accepted: December 7, 2021
Published: December 22, 2021

REFERENCES

1. Nozariasbmarz, A., Collins, H., Dsouza, K., Polash, M.H., Hosseini, M., Hyland, M., Liu, J., Malhotra, A., Ortiz, F.M., and Mohaddes, F. (2020). Review of wearable thermoelectric energy harvesting: from body temperature to electronic systems. Appl. Energy *258*, 114069.

2. Cansiz, M., Altinel, D., and Kurt, G.K. (2019). Efficiency in RF energy harvesting systems: a comprehensive review. Energy *174*, 292–309.

3. Zou, H.X., Zhao, L.C., Gao, Q.H., Zuo, L., Liu, F.R., Tan, T., Wei, K.X., and Zhang, W.M. (2019). Mechanical modulations for enhancing energy harvesting: principles, methods and applications. Appl. Energy *255*, 113871.

4. Mahapatra, B., Patel, K.K., and Patel, P.K. (2021). A review on recent advancement in materials for piezoelectric/triboelectric nanogenerators. Mater. Today Proc. *46*, 5523–5529.

5. Barkas, D.A., Psomopoulos, C., Papageorgas, P., Kalkanis, K., Piromalis, D., and Mouratidis, A. (2019). Sustainable energy harvesting through triboelectric nano–generators: a review of current status and applications. Energy Procedia *157*, 999–1010.

6. Priya, S., Song, H.C., Zhou, Y., Varghese, R., Chopra, A., Kim, S.G., Kanno, I., Wu, L., Ha, D.S., and Ryu, J. (2019). A review on piezoelectric energy harvesting: materials, methods, and circuits. Energy Harvesting Syst. *4*, 3–39.

7. Sezer, N., and Koç, M. (2021). A comprehensive review on the state-of-the-art of piezoelectric energy harvesting. Nano Energy *80*, 105567.

8. Khalid, S., Raouf, I., Khan, A., Kim, N., and Kim, H.S. (2019). A review of human-powered energy harvesting for smart electronics: recent progress and challenges. Int. J. Precis. Eng. Manuf. Green Technol. *6*, 821–851.

9. Shi, Q., He, T., and Lee, C. (2019). More than energy harvesting–combining triboelectric nanogenerator and flexible electronics technology for enabling novel micro-/nano-systems. Nano Energy *57*, 851–871.

10. Safaei, M., Sodano, H.A., and Anton, S.R. (2019). A review of energy harvesting using piezoelectric materials: state-of-the-art a decade later (2008–2018). Smart Mater. Struct. *28*, 113001.

11. Yan, X., Cui, X., Li, B., and Li, L.S. (2010). Large, solution-processable graphene quantum dots as light absorbers for photovoltaics. Nano Lett. *10*, 1869–1873.

12. Frischmann, P.D., Mahata, K., and Würthner, F. (2013). Powering the future of molecular artificial photosynthesis with light-harvesting metallosupramolecular dye assemblies. Chem. Soc. Rev. *42*, 1847–1870.

13. Blackburn, J.L., Ferguson, A.J., Cho, C., and Grunlan, J.C. (2018). Carbon-nanotube-based thermoelectric materials and devices. Adv. Mater. *30*, 1704386.

14. Pandya, S., Wilbur, J., Kim, J., Gao, R., Dasgupta, A., Dames, C., and Martin, L.W. (2018). Pyroelectric energy conversion with large energy and power density in relaxor ferroelectric thin films. Nat. Mater. *17*, 432–438.

15. Baik, J.M., and Lee, J.P. (2019). Strategies for ultrahigh outputs generation in triboelectric energy harvesting technologies: from fundamentals to devices. Sci. Technol. Adv. Mater. *20*, 927–936.

16. Esmaeeli, R., Aliniagerdroudbari, H., Hashemi, S.R., Nazari, A., Alhadri, M., Zakri, W., Mohammed, A.H., Batur, C., and Farhad, S. (2019). A rainbow piezoelectric energy harvesting system for intelligent tire monitoring applications. J. Energy Resour. Technol. *141*, 062007.

17. Sarker, M.R., Julai, S., Sabri, M.F.M., Said, S.M., Islam, M.M., and Tahir, M. (2019). Review of piezoelectric energy harvesting system and application of optimization techniques to

enhance the performance of the harvesting system. Sens. Actuators A Physiol. *300*, 111634.

18. Han, M., Wang, H., Yang, Y., Liang, C., Bai, W., Yan, Z., Li, H., Xue, Y., Wang, X., and Akar, B. (2019). Three-dimensional piezoelectric polymer microsystems for vibrational energy harvesting, robotic interfaces and biomedical implants. Nat. Electron. *2*, 26–35.

19. Siddique, A.R.M., Mahmud, S., and Van Heyst, B. (2015). A comprehensive review on vibration based micro power generators using electromagnetic and piezoelectric transducer mechanisms. Energy Convers. Manage. *106*, 728–747.

20. Wang, H., Jasim, A., and Chen, X. (2018). Energy harvesting technologies in roadway and bridge for different applications–a comprehensive review. Appl. Energy *212*, 1083–1094.

21. Abdelkareem, M.A., Xu, L., Ali, M.K.A., Elagouz, A., Mi, J., Guo, S., Liu, Y., and Zuo, L. (2018). Vibration energy harvesting in automotive suspension system: a detailed review. Appl. Energy *229*, 672–699.

22. Donelan, J.M., Li, Q., Naing, V., Hoffer, J.A., Weber, D.J., and Kuo, A.D. (2008). Biomechanical energy harvesting: generating electricity during walking with minimal user effort. Science *319*, 807–810.

23. Su, Y., Wen, X., Zhu, G., Yang, J., Chen, J., Bai, P., Wu, Z., Jiang, Y., and Wang, Z.L. (2014). Hybrid triboelectric nanogenerator for harvesting water wave energy and as a self-powered distress signal emitter. Nano Energy *9*, 186–195.

24. Brenes, A., Morel, A., Gibus, D., Yoo, C.S., Gasnier, P., Lefeuvre, E., and Badel, A. (2020). Large-bandwidth piezoelectric energy harvesting with frequency-tuning synchronized electric charge extraction. Sens. Actuators A Physiol. *302*, 111759.

25. Chen, C., Sharafi, A., and Sun, J.Q. (2020). A high density piezoelectric energy harvesting device from highway traffic–Design analysis and laboratory validation. Appl. Energy *269*, 115073.

26. Moss, S.D., Payne, O.R., Hart, G.A., and Ung, C. (2015). Scaling and power density metrics of electromagnetic vibration energy harvesting devices. Smart Mater. Struct. *24*, 023001.

27. Zhang, Y., Wang, T., Luo, A., Hu, Y., Li, X., and Wang, F. (2018). Micro electrostatic energy harvester with both broad bandwidth and high normalized power density. Appl. Energy *212*, 362–371.

28. Zhang, Y., Wang, T., Zhang, A., Peng, Z., Luo, D., Chen, R., and Wang, F. (2016). Electrostatic energy harvesting device with dual resonant structure for wideband random vibration sources at low frequency. Rev. Sci. Instrum. *87*, 125001.

29. Kim, T.Y., Kim, S.K., and Kim, S.W. (2018). Application of ferroelectric materials for improving output power of energy harvesters. Nano Converg. *5*, 30.

30. Karami, M.A., and Inman, D.J. (2011). Analytical modeling and experimental verification of the vibrations of the zigzag microstructure for energy harvesting. J. Vib. Acoust. *133*, 011002.

31. Kim, S.B., Park, H., Kim, S.H., Wikle, H.C., Park, J.H., and Kim, D.J. (2012). Comparison of MEMS PZT cantilevers based on d_{31} and d_{33} modes for vibration energy harvesting. J. Microelectromech. Syst. *22*, 26–33.

32. Gao, X., Wu, J., Yu, Y., Chu, Z., Shi, H., and Dong, S. (2018). Giant piezoelectric coefficients in relaxor piezoelectric ceramic PNN-PZT for vibration energy harvesting. Adv. Funct. Mater. *28*, 1706895.

33. Shahab, S., Zhao, S., and Erturk, A. (2018). Soft and hard piezoelectric ceramics and single crystals for random vibration energy harvesting. Energy Technol. *6*, 935–942.

34. Yang, Z., and Zu, J. (2016). Comparison of PZN-PT, PMN-PT single crystals and PZT ceramic for vibration energy harvesting. Energy Convers. Manage. *122*, 321–329.

35. Lin, Y., Liu, Y., and Sodano, H.A. (2009). Hydrothermal synthesis of vertically aligned lead zirconate titanate nanowire arrays. Appl. Phys. Lett. *95*, 122901.

36. Nafari, A., Bowland, C.C., and Sodano, H.A. (2017). Ultra-long vertically aligned lead titanate nanowire arrays for energy harvesting in extreme environments. Nano Energy *31*, 168–173.

37. Harstad, S., D'Souza, N., Soin, N., El Gendy, A.A., Gupta, S., Pecharsky, V.K., Shah, T., Siores, E., and Hadimani, R.L. (2017). Enhancement of β-phase in PVDF films embedded with ferromagnetic Gd_5Si_4 nanoparticles for piezoelectric energy harvesting. AIP Adv. *7*, 056411.

38. Datta, A., Choi, Y.S., Chalmers, E., Ou, C., and Kar-Narayan, S. (2017). Piezoelectric nylon-11 nanowire arrays grown by template wetting for vibrational energy harvesting applications. Adv. Funct. Mater. *27*, 1604262.

39. Qian, J., He, J., Qian, S., Zhang, J., Niu, X., Fan, X., Wang, C., Hou, X., Mu, J., and Geng, W. (2020). A nonmetallic stretchable nylon-modified high performance triboelectric nanogenerator for energy harvesting. Adv. Funct. Mater. *30*, 1907414.

40. Xu, L., Xu, L., Luo, J., Yan, Y., Jia, B.E., Yang, X., Gao, Y., and Wang, Z.L. (2020). Hybrid all-in-one power source based on high-performance spherical triboelectric nanogenerators for harvesting environmental energy. Adv. Energy Mater. *10*, 2001669.

41. Fan, F.R., Tian, Z.Q., and Wang, Z.L. (2012). Flexible triboelectric generator. Nano Energy *1*, 328–334.

42. Lin, Z., Chen, J., and Yang, J. (2016). Recent progress in triboelectric nanogenerators as a renewable and sustainable power source. J. Nanomater. *2016*, 5651613.

43. Wang, Z.L. (2017). On Maxwell's displacement current for energy and sensors: the origin of nanogenerators. Mater. Today *20*, 74–82.

44. Hinchet, R., Yoon, H.-J., Ryu, H., Kim, M.K., Choi, E.K., Kim, D.S., and Kim, S.W. (2019). Transcutaneous ultrasound energy harvesting using capacitive triboelectric technology. Science *365*, 491–494.

45. Wang, J., Wu, C., Dai, Y., Zhao, Z., Wang, A., Zhang, T., and Wang, Z.L. (2017). Achieving ultrahigh triboelectric charge density for efficient energy harvesting. Nat. Commun. *8*, 88.

46. Choi, Y.S., Kim, S.K., Smith, M., Williams, F., Vickers, M.E., Elliott, J.A., and Kar-Narayan, S. (2020). Unprecedented dipole alignment in α-phase nylon-11 nanowires for high-performance energy-harvesting applications. Sci. Adv. *6*, eaay5065.

47. Choi, Y.S., Jing, Q., Datta, A., Boughey, C., and Kar-Narayan, S. (2017). A triboelectric generator based on self-poled Nylon-11 nanowires fabricated by gas-flow assisted template wetting. Energy Environ. Sci. *10*, 2180–2189.

48. Kim, J., Ryu, H., Lee, J.H., Khan, U., Kwak, S.S., Yoon, H.J., and Kim, S.W. (2020). High permittivity $CaCu_3Ti_4O_{12}$ particle-induced internal polarization amplification for high performance triboelectric nanogenerators. Adv. Energy Mater. *10*, 1903524.

49. Xu, Y. (2013). Ferroelectric materials and their applications (Elsevier).

50. Martin, L.W., and Rappe, A.M. (2016). Thin-film ferroelectric materials and their applications. Nat. Rev. Mater. *2*, 16087.

51. Cross, L.E. (1996). Ferroelectric materials for electromechanical transducer applications. Mater. Chem. Phys. *43*, 108–115.

52. Bakshi, A.N., Moghal, A.A.B., Madhar, N.A., Patel, S., and Vaish, R. (2015). Effect of stress on energy conversion and storage characteristics of (1-xy) PIN-xPMN-yPT single crystals. Ferroelectr. Lett. Sect. *42*, 107–114.

53. Chauhan, A., Patel, S., and Vaish, R. (2016). Enhanced mechanical energy conversion potential in ferroelectric single crystals. Mater. Technol. *31*, 274–280.

54. Münch, I., Krauß, M., Landis, C.M., and Huber, J.E. (2011). Domain engineered ferroelectric energy harvesters on a substrate. J. Appl. Phys. *109*, 104106.

55. Muench, I., Krauss, M., Wagner, W., and Kamlah, M. (2012). Ferroelectric nanogenerators coupled to an electric circuit for energy harvesting. Smart Mater. Struct. *21*, 115026.

56. Balakrishna, A.R., and Huber, J.E. (2016). Nanoscale domain patterns and a concept for an energy harvester. Smart Mater. Struct. *25*, 104001.

57. Wang, D., Wang, L., and Melnik, R. (2017). Vibration energy harvesting based on stress-induced polarization switching: a phase field approach. Smart Mater. Struct. *26*, 065022.

58. Wang, D., Melnik, R., and Wang, L. (2018). Material influence in newly proposed ferroelectric energy harvesters. J. Intell. Mater. Syst. Struct. *29*, 3305–3316.

59. Kang, W., and Huber, J.E. (2019). Prospects for energy harvesting using ferroelectric/ferroelastic switching. Smart Mater. Struct. *28*, 024002.

60. Behlen, L., Warkentin, A., and Ricoeur, A. (2021). Exploiting ferroelectric and ferroelastic effects in piezoelectric energy harvesting: theoretical studies and parameter optimization. Smart Mater. Struct. *30*, 035031.

61. Ma, W., and Cross, L.E. (2006). Flexoelectricity of barium titanate. Appl. Phys. Lett. *88*, 232902.

62. Zhu, R., Wang, Z., Ma, H., Yuan, G., Wang, F., Cheng, Z., and Kimura, H. (2018). Poling-free energy harvesters based on robust self-poled ferroelectric fibers. Nano Energy *50*, 97–105.

63. Maamer, B., Boughamoura, A., El Bab, A.M.F., Francis, L.A., and Tounsi, F. (2019). A review on design improvements and techniques for mechanical energy harvesting using piezoelectric and electromagnetic schemes. Energy Convers. Manage. *199*, 111973.

64. De Marqui, C., Jr., Erturk, A., and Inman, D.J. (2009). An electromechanical finite element model for piezoelectric energy harvester plates. J. Sound Vibrat. *327*, 9–25.

65. Khazaee, M., Rezaniakolaie, A., and Rosendahl, L. (2020). A broadband macro-fiber-composite piezoelectric energy harvester for higher energy conversion from practical wideband vibrations. Nano Energy *76*, 104978.

66. Jin, W., Wang, Z., Huang, H., Hu, X., He, Y., Li, M., Li, L., Gao, Y., Hu, Y., and Gu, H. (2018). High-performance piezoelectric energy harvesting of vertically aligned Pb (Zr, Ti) O_3 nanorod arrays. RSC Adv. *8*, 7422–7427.

67. Xu, S., Hansen, B.J., and Wang, Z.L. (2010). Piezoelectric-nanowire-enabled power source for driving wireless microelectronics. Nat. Commun. *1*, 93.

68. Yan, X., Zheng, M., Hou, Y., Zhu, M., and Yan, H. (2018). High energy conversion efficiency in Mn-modified $Ba_{0.9}Ca_{0.1}Ti_{0.93}Zr_{0.07}O_3$ lead-free energy harvester. J. Am. Ceram. Soc. *101*, 2330–2338.

69. Yi, Z., Yang, B., Li, G., Liu, J., Chen, X., Wang, X., and Yang, C. (2017). High performance bimorph piezoelectric MEMS harvester via bulk PZT thick films on thin beryllium-bronze substrate. Appl. Phys. Lett. *111*, 013902.

70. Najafi, K., Galchev, T., Aktakka, E.E., Peterson, R.L., and McCullagh, J. (2011). Microsystems for energy harvesting. In 2011 16th International Solid-State Sensors, Actuators and Microsystems Conference (IEEE), pp. 1845–1850.

71. Won, S.S., Seo, H., Kawahara, M., Glinsek, S., Lee, J., Kim, Y., Jeong, C.K., Kingon, A.I., and Kim, S.H. (2019). Flexible vibrational energy harvesting devices using strain-engineered perovskite piezoelectric thin films. Nano Energy *55*, 182–192.

72. Xu, C., Ren, B., Di, W., Liang, Z., Jiao, J., Li, L., Li, L., Zhao, X., Luo, H., and Wang, D. (2012). Cantilever driving low frequency piezoelectric energy harvester using single crystal material 0.71 Pb ($Mg_{1/3}Nb_{2/3}$) O_3-0.29 $PbTiO_3$. Appl. Phys. Lett. *101*, 033502.

73. Zhu, G., Zhou, Y.S., Bai, P., Meng, X.S., Jing, Q., Chen, J., and Wang, Z.L. (2014). A shape-adaptive thin-film-based approach for 50% high-efficiency energy generation through micro-grating sliding electrification. Adv. Mater. *26*, 3788–3796.

74. Salauddin, M., Toyabur, R., and Park, J. (2018). A free motion driven electromagnetic and triboelectric hybridized nanogenerator for scavenging low frequency vibrations. In 2018 IEEE Micro Electro Mechanical Systems Conference (IEEE), pp. 233–236.

75. Tayyab, M., Wang, J., Wang, J., Maksutoglu, M., Yu, H., Sun, G., Yildiz, F., Eginligil, M., and Huang, W. (2020). Enhanced output in polyvinylidene fluoride nanofibers based triboelectric nanogenerator by using printer ink as nano-fillers. Nano Energy *77*, 105178.

76. Mao, Y., Geng, D., Liang, E., and Wang, X. (2015). Single-electrode triboelectric nanogenerator for scavenging friction energy from rolling tires. Nano Energy *15*, 227–234.

77. Hwang, S.C., Lynch, C.S., and McMeeking, R.M. (1995). Ferroelectric/ferroelastic interactions and a polarization switching model. Acta Metall. Mater. *43*, 2073–2084.

78. Lynch, C.S. (1996). The effect of uniaxial stress on the electro-mechanical response of 8/65/35 PLZT. Acta Mater. *44*, 4137–4148.

79. Huber, J.E., Hofmann, F., Barhli, S., Marrow, T.J., and Hildersley, C. (2017). Observation of crack growth in a polycrystalline ferroelectric by synchrotron X-ray diffraction. Scr. Mater. *140*, 23–26.

80. Hocine, S., Van Swygenhoven, H., Van Petegem, S., Chang, C.S.T., Maimaitiyili, T., Tinti, G., Sanchez, D.F., Grolimund, D., and Casati, N. (2020). Operando X-ray diffraction during laser 3D printing. Mater. Today *34*, 30–40.